

1 Pixel Purity Index Algorithm and n-Dimensional Visualization  
2 for ETM+ Image Analysis: A Case of District Vehari

3 Dr. Farooq Ahmad<sup>1</sup>

4 <sup>1</sup> University of the Punjab, Lahore, Pakistan.

5 *Received: 14 December 2011 Accepted: 1 January 2012 Published: 15 January 2012*

6

---

7 **Abstract**

8 The hyperspectral image analysis technique, one of the most advanced remote sensing tools,  
9 has been used as a possible means of identifying from a single pixel or in the field of view of  
10 the sensor. An important problem in hyperspectral image processing is to decompose the  
11 mixed pixels into the information that contribute to the pixel, endmember, and a set of  
12 corresponding fractions of the spectral signature in the pixel, abundances, and this problem is  
13 known as un-mixing. The effectiveness of the hyperspectral image analysis technique used in  
14 this study lies in their ability to compare a pixel spectrum with the spectra of known pure  
15 vegetation, extracted from the spectral endmember selection procedures, including the  
16 reflectance calibration of Landsat ETM+ image using ENVI software, minimum noise fraction  
17 (MNF), pixel purity index (PPI), and n-dimensional visualization. The Endmember  
18 extraction is one of the most fundamental and crucial tasks in hyperspectral data exploitation,  
19 an ultimate goal of an endmember extraction algorithm is to find the purest form of spectrally  
20 distinct resource information of a scene. The endmember extraction tendency to the type of  
21 endmembers being derived, and the number of endmembers, estimated by an algorithm, with  
22 respect to the number of spectral bands, and the number of pixels being processed, also the  
23 required input data, and the kind of noise, if any, in the signal model surveying done. Results  
24 of the present study using the hyperspectral image analysis technique ascertain that Landsat  
25 ETM+ data can be used to generate valuable vegetative information for the District Vehari,  
26 Punjab Province, Pakistan.

27

---

28 **Index terms**— Algorithm, endmember, fraction, LandsatMNF, n-dimension, PPI, remote sensing.

29 **1 I. Introduction**

30 The recent developments in remote sensing technology have witnessed two major trends in sensor improvement  
31 (Qiu et al., 2006). The hyperspectral imaging (Shippert, 2003) is concerned with the measurement, analysis,  
32 and interpretation of spectra acquired from a given scene at a short, medium or long distance by an airborne  
33 or satellite sensor (Goetz et al., 1985; Aspinall et al., 2002). The pixel purity index (González et al., 2010; Pal  
34 et al., 2011) allows for spatial data reduction. The pixels in the image that represent the 'most pure' spectral  
35 signatures are identified and subset from the mass majority of pixels representing mixed pixels. A 'pure' pixel,  
36 also known as an endmember (Nascimento and Dias, 2005), can be envisioned as a homogenous area greater in  
37 spatial extent than the image pixel size, so that the recorded signal for that pixel represents a spectral profile for  
38 single surface information (Boardman, 1993; Boardman et al., 1995). It assumes that the pixel-to-pixel variability  
39 in a scene results from varying proportions of spectral endmembers (Rogge et al., 2007). The spectrum of a mixed  
40 pixel can be calculated as a linear combination of the endmember spectra weighted by the area coverage of each  
41 endmember within the pixel, if the scattering and absorption of electromagnetic radiation is derived from a single

### 3 III. RESULTS

---

42 component on the surface (Keshava and Mustard, 2002; Rogge et al., 2007). Image endmembers are pixel spectra  
43 that lie at the vertices of the image simplex in n-dimensional space. Imagery may provide similarly meaningful  
44 endmembers that can be considered 'pure' or relatively 'pure' spectra, meaning that little or no mixing with  
45 other endmembers has occurred within a given pixel (Rogge et al., 2007). A mixed pixel is a picture element  
46 representing an area occupied by more than one ground cover type (Mozaffar et al., 2008). Spectral unmixing  
47 represents a significant step in the evolution of remote decompositional analysis that began with multispectral  
48 sensing (Shippert, 2003). It is a consequence of collecting data in greater and greater quantities and the desire  
49 to extract more detailed information about the resource composition ??Keshava and Mustard, 2002). Spectral  
50 analysis extracts useful information might have missed otherwise from the raw pixel values of medium and high  
51 resolution imagery and can reveal hidden information locked in the pixels of imagery ??Keshava and Mustard,  
52 2002;Shippert, 2003).

53 The hyperspectral imagery provides opportunities to extract more detailed information than is possible using  
54 traditional multispectral data. The future of hyperspectral remote sensing is promising (Shippert, 2003).  
55 As newly commissioned hyperspectral sensors provide more imagery alternatives, and newly developed image  
56 processing algorithms provide more analytical tools, hyperspectral remote sensing is positioned to become one of  
57 the core technologies for geospatial research (Shippert, 2004), exploration, and monitoring.

58 Hyperspectral images have been used to detect soil properties including moisture, organic content, and

## 59 2 Research Design and Methods

60 In this research paper Landsat ETM+ scene 2003 for the District Vehari (path 150, row 39) was used for  
61 hyperspectral image analysis. In order to use this scene, several steps were followed to prepare for an accurate  
62 extraction of vegetation endmember. These vital steps are: image registration, geometric correction, radiometric  
63 enhancement, and histogram equalization as discussed by Macleod and Congalton (1998), Mahmoodzadeh (2007)  
64 and Al-Awadhi et al., 2011. The scene was corrected and geo-referenced using projection UTM, zone 43 and  
65 datum WGS 84. Atmospheric correction operation was performed using ENVI software. Further, Minimum  
66 Noise Fraction (MNF), Pixel Purity Index (PPI), n-Dimensional Visualizer (n-DV) and Endmember Extraction  
67 technique has been used for hyperspectral image analysis (Figure 1).

68 The Pixel Purity Index (PPI) technique was adopted using ENVI 'automated spectral hourglass' application  
69 upon ETM+ image. The PPI was applied upon the full scene of the district. In this experiment 22,948,704  
70 pixels were operated (Figure 3 The hyperspectral imaging, also known as imaging spectrometry, is now a  
71 reasonably familiar concept in the world of remote sensing. Hyperspectral images are spectrally providing ample  
72 spectral information (Shippert, 2003) to identify and distinguish between spectrally similar resource information.  
73 Consequently, hyperspectral imagery provides the potential for more accurate and detailed information extraction  
74 than is possible with other types of remotely sensed data (Shippert, 2004). Standard multispectral image  
75 processing techniques were generally developed to classify multispectral images into broad categories of surface  
76 condition. Hyperspectral imagery provides an opportunity for more detailed image analysis. Boardman (1993)  
77 and Boardman et al. (1995) were among the first to develop and commercialize a sequence of algorithms  
78 specifically designed to extract detailed information from hyperspectral imagery (Shippert, 2004). ENVI tools,  
79 applicable to a variety of applications, distinguish and identify the unique resource information present in the  
80 scene and map them throughout the image (Research System, Inc., 2004).

## 81 3 III. Results

82 The hyperspectral imaging is a new emerging technology in remote sensing which generates hundreds of images,  
83 at different wavelength channels, for the same area on the surface of the Earth (Goetz et al., 1985 A region  
84 from 0.38 to 2.5 ?m or 380 nm to 2500 nm using two hundred twenty four spectral channels, at nominal spectral  
85 resolution of 10 nm (González et al., 2010).

86 The Pixel Purity Index (PPI) is a new automated procedure in the hyperspectral analysis process (Boardman,  
87 1993;Boardman et al., 1995) for defining potential image endmember spectra (Bateson and Curtiss, 1996) for  
88 spectral unmixing ??Lillesand and Kiefer, 2000). When image spectra are treated as points in n-dimensional  
89 spectral space, endmember spectra should lie along the margins of the data cloud (MicroImages, Inc., 1999;  
90 Berman et al., 2004). The PPI creates a large number of randomly oriented test vectors anchored at the origin  
91 of the coordinate space. The spectral points are projected onto each test vector, and spectra within a threshold  
92 distance of the minimum and maximum projected values are flagged as extreme (Nascimento and Dias, 2005).  
93 As directions are tested, the process tallies the number of times an image cell is found to be extreme (Miao and  
94 Qi, 2007). Cells with high values in the resulting PPI raster should correspond primarily to 'edge' spectra . The  
95 PPI raster then can be used as a mask to control input to the n-dimensional visualizer (MicroImages, Inc., 1999;  
96 Zhang et al., 2008).

97 The most commonly used endmember extraction (Figure 5, 6 and Table 1, 2) tool is pixel purity index, which  
98 searches for vertices that define the data volume in n-dimensional space (Rogge et al., 2007). Commonly the  
99 first step of PPI is to apply MNF (Lee et al., 1990) to reduce the dimensionality of the data set ??Green et al.,  
100 1988;Rogge et al., 2007). The MNF transform is used to determine the inherent dimensionality of image data, to  
segregate noise in the data, and to reduce the computational requirements for subsequent processing (Boardman

102 and Kruse, 1994). The transformation based on an estimated noise covariance matrix, decorrelates and rescales  
103 the noise in the data ??Research Systems, Inc., 2003;2004). This step results in transformed data in which the  
104 noise has unit variance and no band-to-band correlations. For the purposes of further spectral processing, the  
105 inherent dimensionality of the data is determined by examination of the final eigenvalues and the associated  
106 images. The data space can be divided into two parts: one part associated with large eigenvalues and coherent  
107 eigenimages, and a complementary part with near-unity eigenvalues and noise-dominated images. By using only  
108 the coherent portions, the noise is separated from the data, thus improving spectral processing results ??Research  
109 Systems, Inc., 2001;2004).

110 Spectra can be thought of as points in an n-dimensional scatter plot, where n is the number of bands (Boardman  
111 et al., 1995). The coordinates of the points in n-space consist of 'n' values that are simply the spectral radiance  
112 or reflectance values in each band for a given pixel. The distribution of these points in n-space can be used to  
113 estimate the number of spectral endmembers and their pure spectral signatures (Research Systems, Inc., 2001).  
114 The scatter plot (Figure 7) is an important tool for exploring an image and helping to understand some of the  
115 spectral characteristics of features in an image. The two dimensional scatter plotting tool allows comparing not  
116 only the relationship between the data values in two selected bands but also the spatial distribution in the image  
117 of pixels in any area of the scatter plot. This combined functionality provides a very simple, twoband, interactive  
118 classification of image data (Research Systems, Inc., 2004).

119 Spectral unmixing (Figure ??) algorithms (Lillesand and Kiefer, 2000; Rogge et al., 2006) use a variety of  
120 different statistical procedures to endmember extraction and estimate abundances. Unmixing problem comprises  
121 three sequential steps: dimension reduction, endmember determination, and inversion (Chang and Plaza, 2006).  
122 Because hyperspectral scenes can include extremely large amount of data, some algorithms for spectral unmixing  
123 first use image itself to estimate endmembers present in the scene. The dimension-reduction stage reduces the  
124 dimension of the original data in the scene (Cochrane, 2000;Mozaffar et al., 2008). The noise estimate can come  
125 from one of three sources; from the dark current image acquired with the data, from noise statistics calculated  
126 from the data (Richards and Jia, 1999), or from statistics saved from a previous transform. Both the eigenvalues  
127 and the Minimum Noise Fraction (MNF -Figure 10) images (eigenimages) are used to evaluate the dimensionality  
128 of the data (Qiu et al., 2006). Eigenvalues for bands that contain information will be an order of magnitude  
129 larger than those that contain only noise. The corresponding images will be spatially coherent, while the noise  
130 images will not contain any spatial information (Research Systems, Inc., 2004; Qiu et al., 2006). Processed by  
131 the author.

132 Processed by the author. The Mixture Tuned Matched Filtering (MTMF -Figure 11) algorithm builds upon the  
133 strengths of both matched filtering and spectral unmixing while avoiding the disadvantages of both (Boardman,  
134 1998). Matched filtering performs partial unmixing and identifies abundance of spectral endmembers without  
135 knowing background endmember signatures (Harsanyi and Chang 1994; Boardman et al., 1995). Matched filtering  
136 does not distinguish rare spectral targets very well and assumes an additive signal based upon radio/radar  
137 applications. Spectral unmixing takes advantage of the hyperspectral leverage to solve the linear mixed pixel  
138 problem, but traditional spectral unmixing techniques require knowledge of all of the background endmembers  
139 (Boardman, 1993;Bateson and Curtiss, 1996;Bateson et al., 2000). Incorporating convex geometry concepts,  
140 mixtures must be non-negative and unit-sum helps identify false positives, unrealistic mixtures, and maps subpixel  
141 fractional abundances.

142 The Minimum Noise Fraction (MNF) data reduction transform and Mixture Tuned Matched Filtering (MTMF)  
143 partial unmixing classification algorithm are relatively new image processing techniques that have proven to be  
144 effective target detection tools (Research Systems, Inc., 2004). These techniques allow partial unmixing and  
145 subpixel target abundance estimation, products that cannot be achieved using spectral angle mapping algorithms  
146 (Mundt et al., 2007).

147 The n-dimensional visualizer serves as an interactive tool for multidimensional analysis and identification of  
148 spectral endmembers (Tompkins et al., 1997;Plaza et al., 2002). The data are displayed in a defined number of  
149 dimensions and spectral endmembers are identified as pixels that are located at the corner vertices (Tsai and  
150 Philpot, 1998). The n-dimensional visualizer second round of spatial data reduction designed to identify particular  
151 pixels or group of pixels that represent the purest spectra within the image. These pure spectra are exported  
152 and saved as ROI's that can be used for subsequent image classification techniques.

153 The n-dimensional visualizer was used to interactively locate, identify, and cluster the most spectrally pure  
154 or unique pixels in the image by visualizing those pixels selected from the PPI as points in an multidimensional  
155 scatter plot (Figure 7), where the number of dimensions was defined by the total number of coherent MNF bands  
156 (Boardman, 1993; ??arris, 2006). The advantage of the n-dimensional visualizer was that it allowed visualization  
157 of points in an n-dimensional space, forming a data 'cloud' (Berk et al., 1998; ??arris, 2006).

158 Advantages of this technology include both the qualitative benefits derived from a visual overview, and more  
159 importantly, the quantitative abilities for systematic assessment and monitoring (Shippert, 2003) Pixel Purity  
160 Index Algorithm and N-Dimensional Visualization for ETM+ Image Analysis: A Case of District Vehari

## 161 4 IV. Discussion and Conclusions

162 The potential of hyperspectral remote sensing is exciting; there are special issues that arise with this unique  
163 type of imagery. For example, many hyperspectral analysis algorithms require accurate atmospheric corrections

## 5 V. ACKNOWLEDGEMENTS

---

164 to be performed. To meet this need, sophisticated atmospheric correction algorithms have been developed to  
165 calculate concentrations of atmospheric gases directly from the detailed spectral information contained in the  
166 imagery (Roberts et al., 1993;Cochrane, 2000;Okin et al., 2001; ??iano et al., 2002) itself without additional  
167 ancillary data. These corrections can be performed separately for each pixel because each pixel has a detailed  
168 spectrum associated with it. Several of these atmospheric correction algorithms are available within commercial  
169 image processing software (Shippert, 2004). However, several image analysis algorithms have been successfully  
170 used with uncorrected imagery (Shippert, 2003).

171 The MNF transform applied to the ETM+ data achieved a reasonable separation of coherent signal from  
172 complementary noise, therefore the MNF transformed eigenimages were employed and coupled with pixel purity  
173 index and n-dimensional visualization techniques to facilitate the extraction of the endmembers (Song, 2005;Qiu  
174 et al., 2006). After applying PPI thresholding, the data volume to be analyzed has been effectively reduced (Zhang  
175 et al., 2000). However, it is still possible that many less 'pure' pixels have crept in as candidate endmembers  
176 during the automatic selection process. All the pixels that were previously selected using the PPI thresholding  
177 procedure are displayed as pixel clouds in the ndimensional spectral space (Welch et al., 1998). To make possible  
178 the visualization of a scatter plot with more than two dimensions, the pixel clouds of high dimensions are cast  
179 on the two-dimensional display screen ??Kruse et al., 1993;Tu et al., 1998). To effectively extract endmembers  
180 from high dimensional remote sensing data (Plaza et al., 2004) and to effectively process the data, it is often  
181 necessary that the dimensionality of the original data be decreased and noise in the data be segregated first, so  
182 the visualizing complexity and computational requirement for the subsequent analysis can be reduced ??Kalluri  
183 et al., 2001;Qiu et al., 2006). This is often achieved through applying a minimum noise fraction transform to the  
184 high dimensional data (Qiu et al., 2006).

185 The hyperspectral sensors and analysis have provided more information from remotely sensed imagery than  
186 ever possible before. As new sensors provide more hyperspectral imagery and new image processing algorithms  
187 continue to be developed, hyperspectral imagery (Shippert, 2003) is positioned to become one of the most  
188 common research (Shippert, 2004) employed was implemented based on the comparison of a pixel spectrum with  
189 the spectra of known pure resource information, which can be effectively extracted using endmember selection  
190 procedures such as minimum noise fraction, pixel purity index and ndimensional visualization.

## 191 5 V. Acknowledgements

The 1 2 3

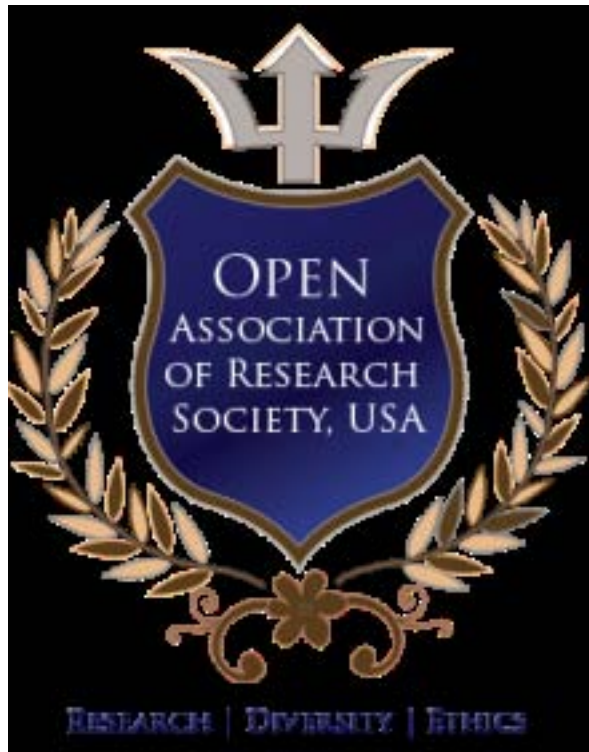


Figure 1:

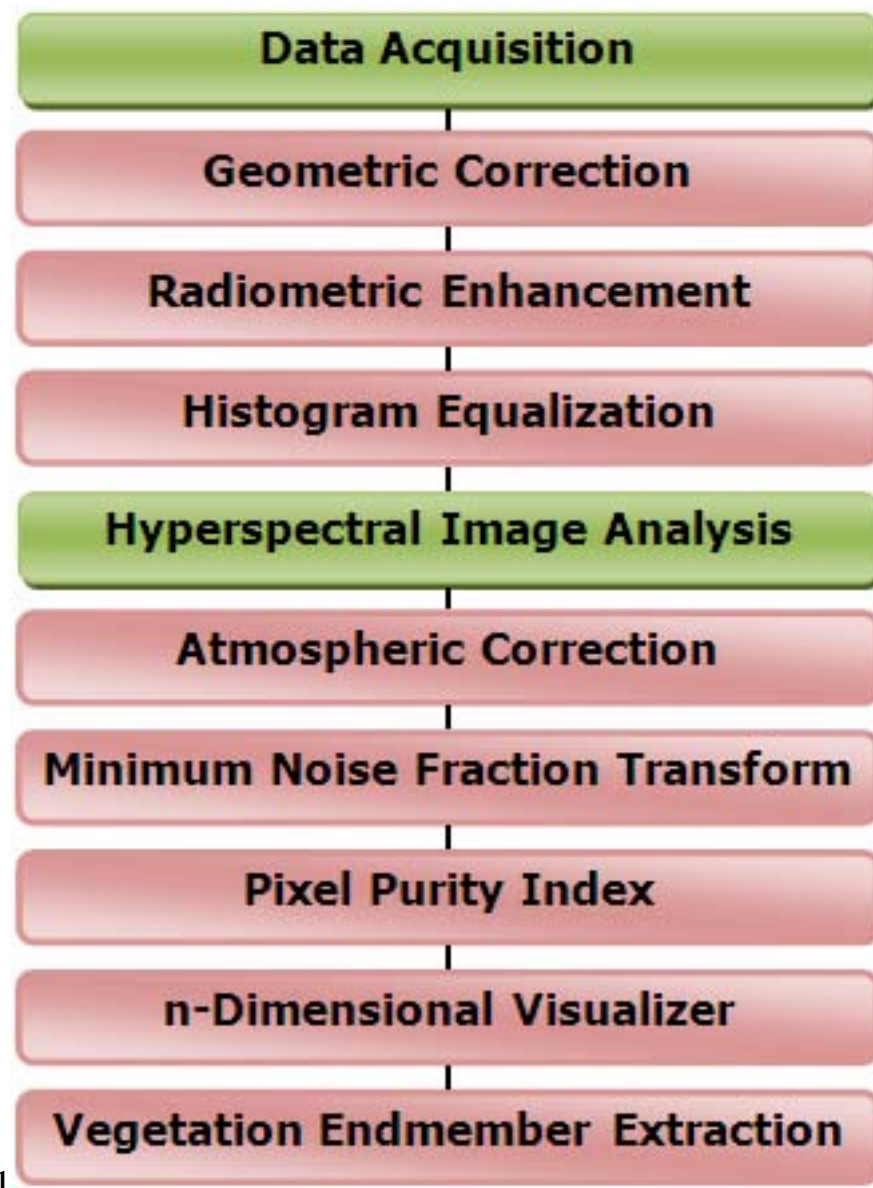


Figure 2: Figure 1 :

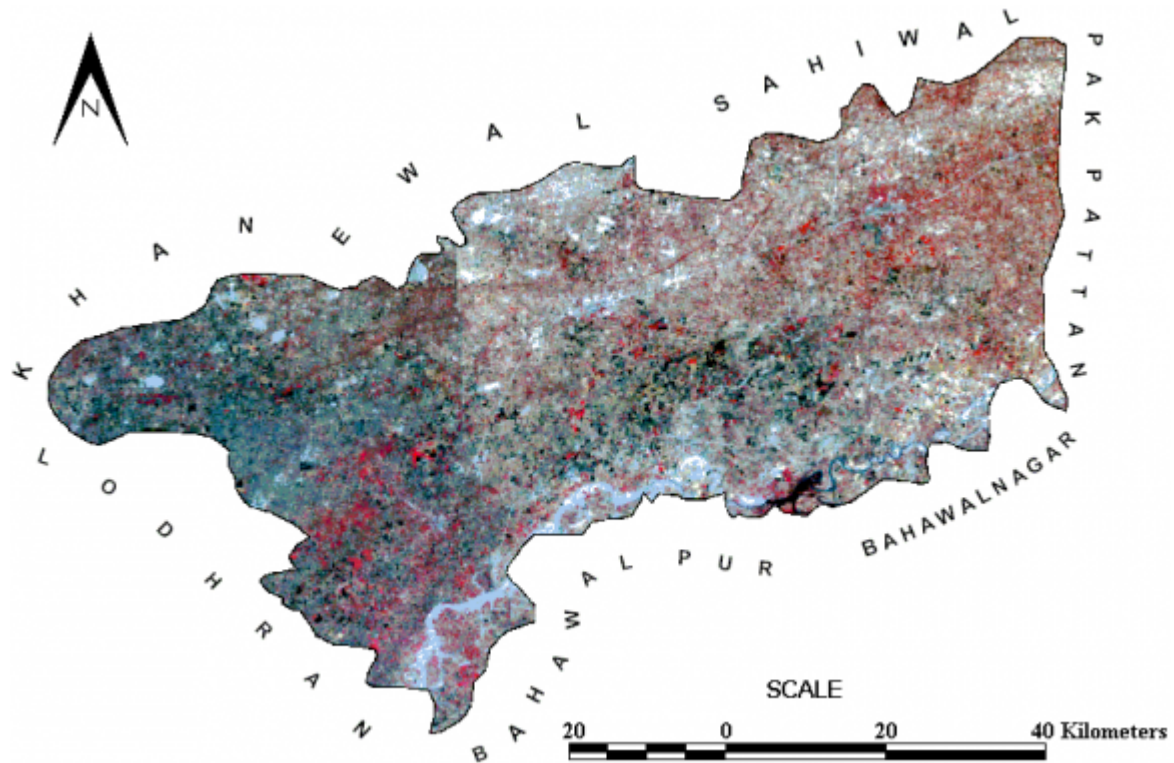
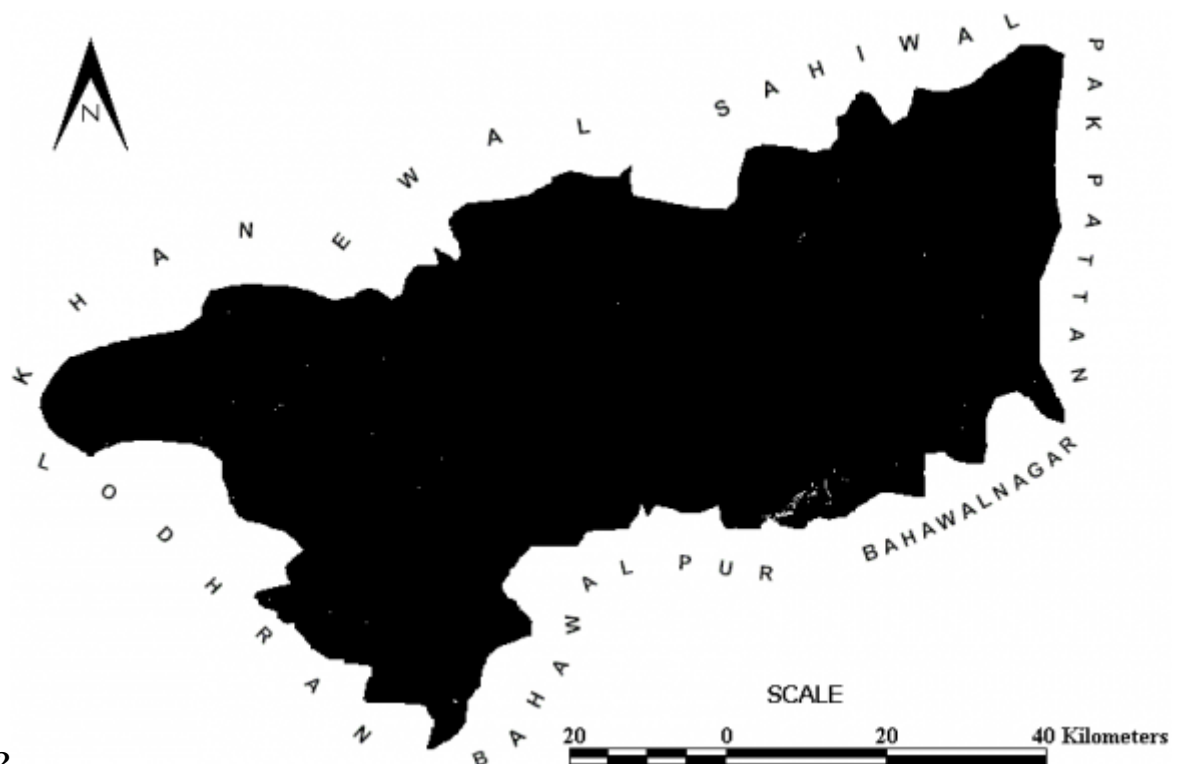


Figure 3:



2

Figure 4: Figure 2 :

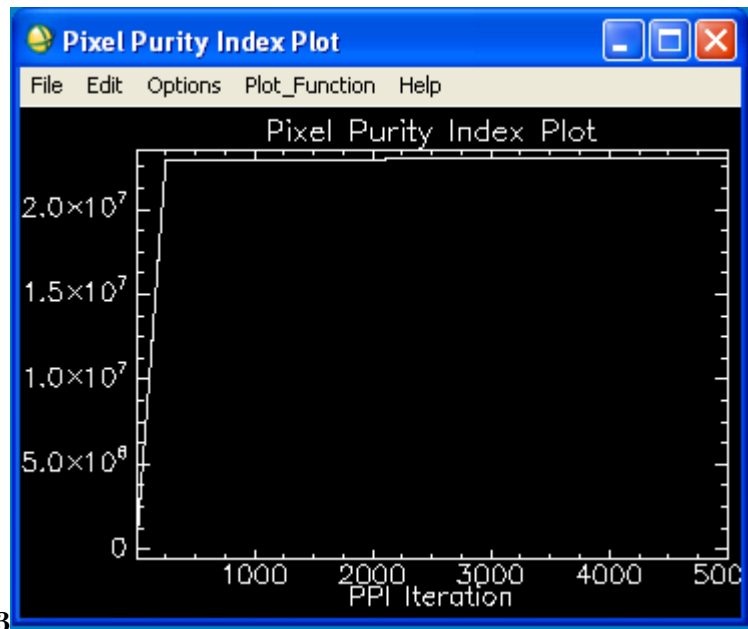


Figure 5: Figure 3 :

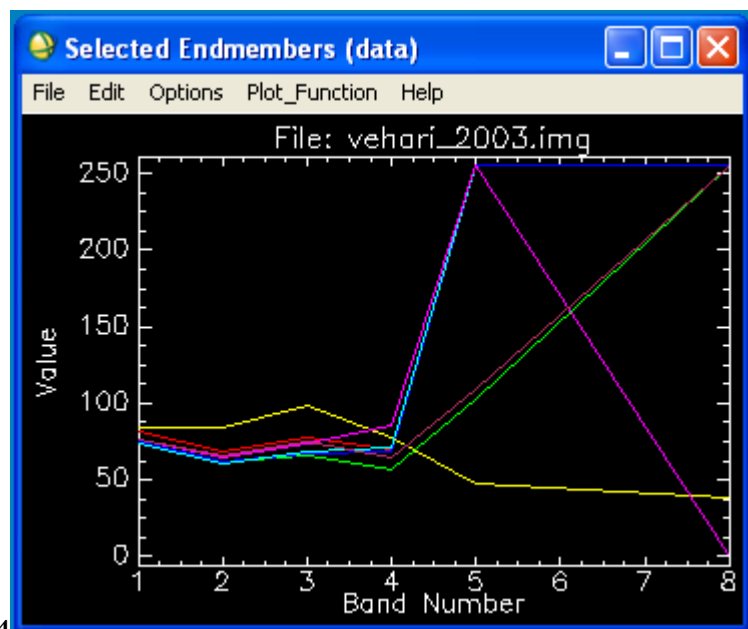


Figure 6: Figure 4 :

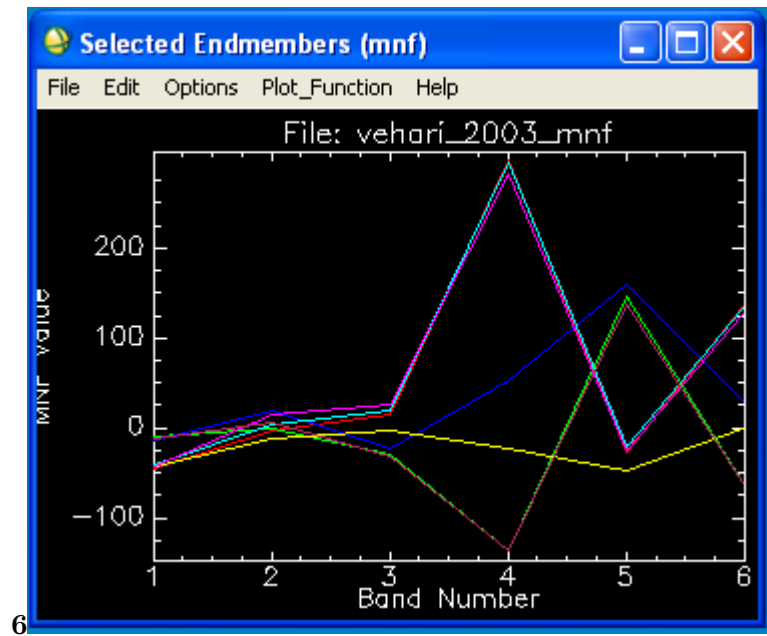


Figure 7: Figure 6 :

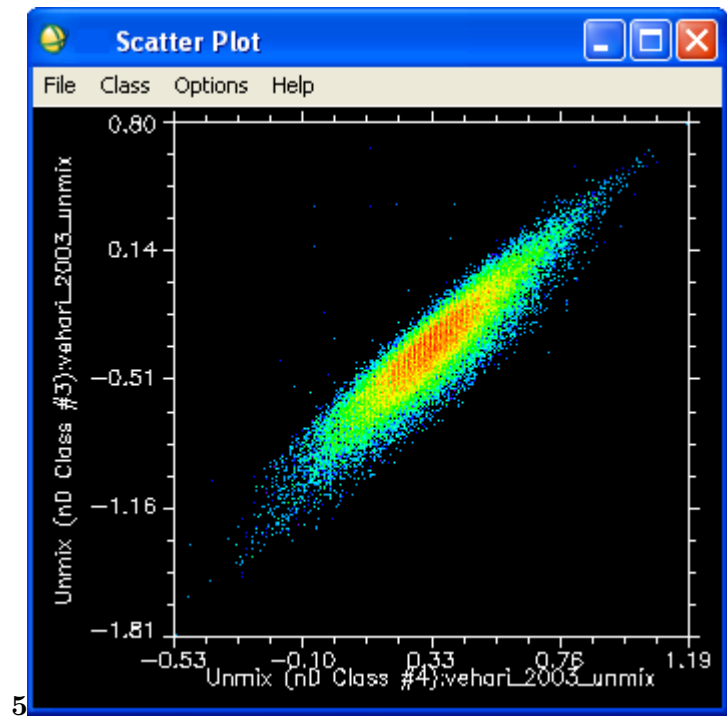


Figure 8: Figure 5 :



Figure 9: Figure 7 :

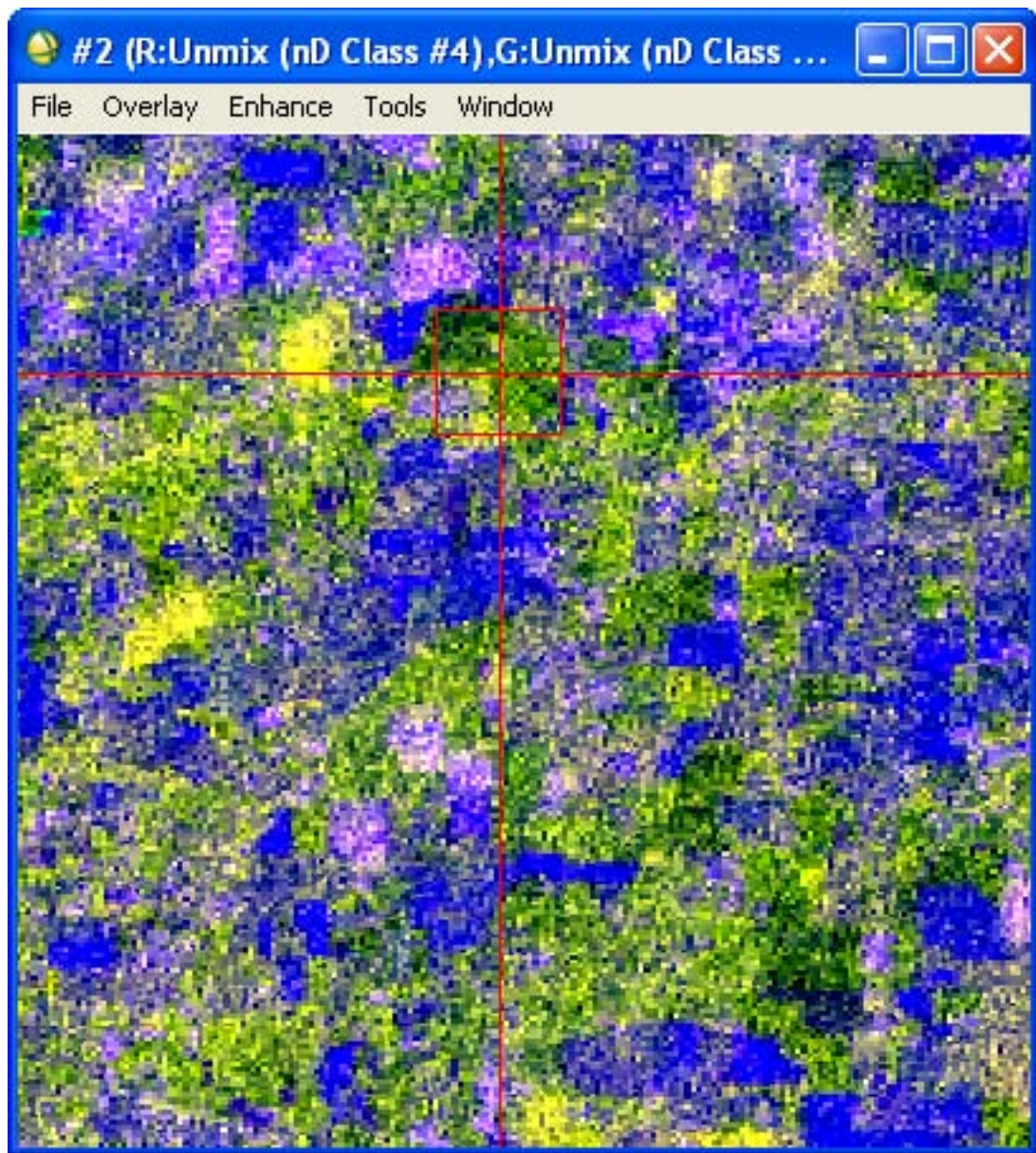


Figure 10:

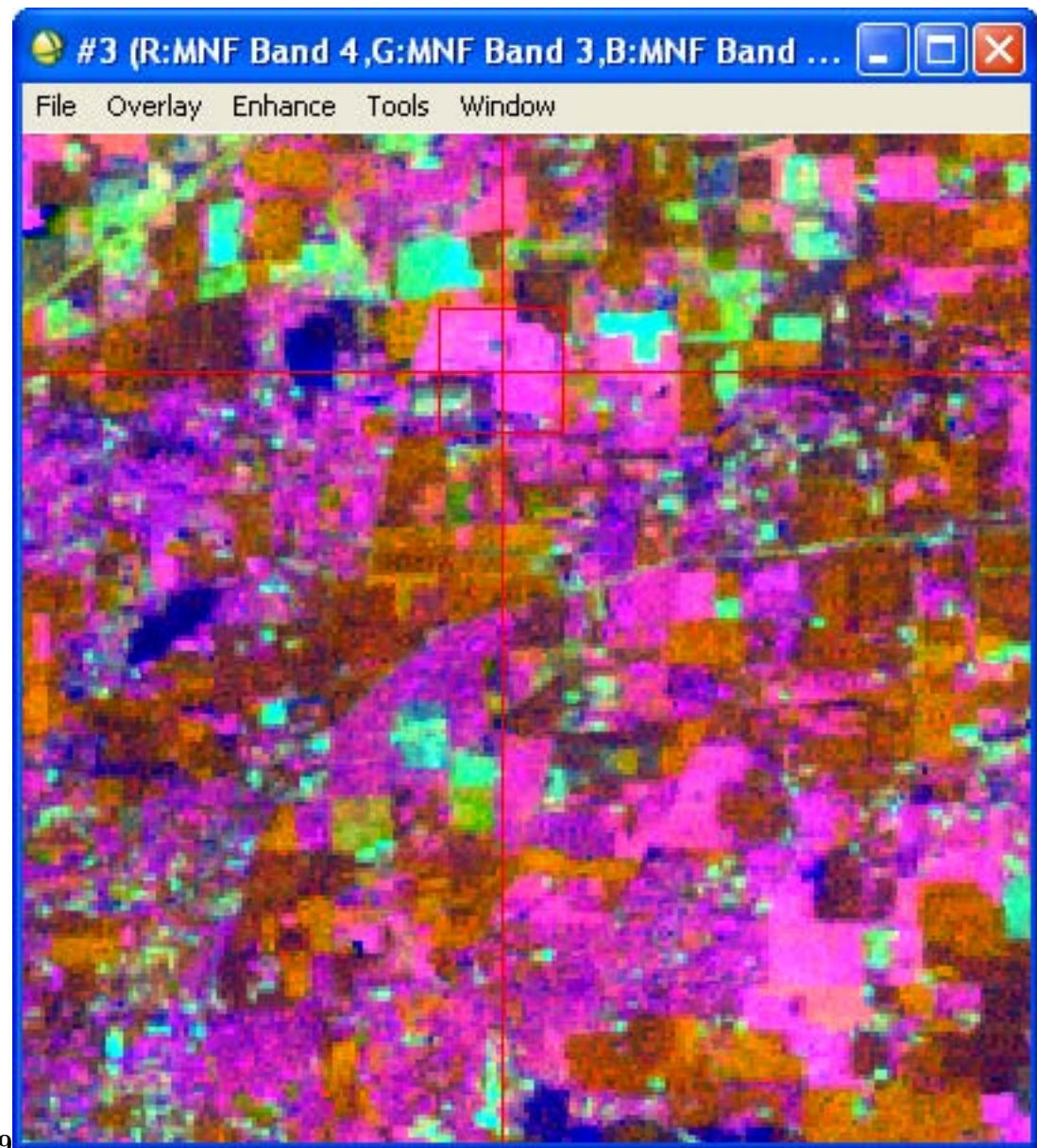


Figure 11: Figure 8 :Figure 9 :

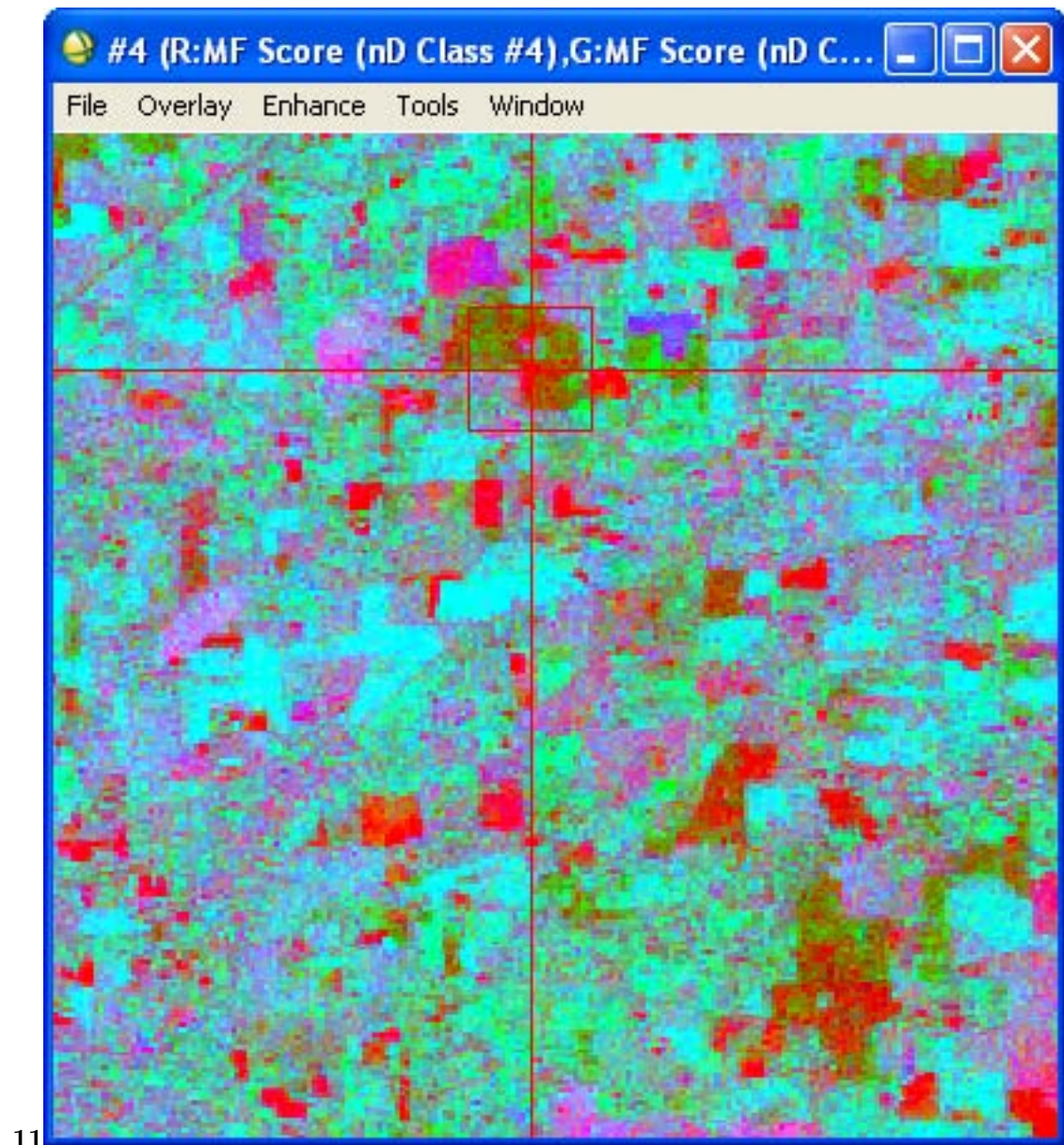


Figure 12: Figure 11 :

---

salinity (Ben-Dor et al., 2002). Vegetation scientists have successfully used hyperspectral imagery to identify vegetation species (Clark and Swayze, 1995), study plant canopy chemistry (Aber and Martin, 1995; Shippert, 2003), and detect vegetation stress.

a) Study Area

The District Vehari (Figure 2 and 8) lies between  $29^{\circ} 36'$  and  $30^{\circ} 22'$  North latitude and  $71^{\circ} 44'$  and  $72^{\circ} 53'$  East longitude (GOP, 2000). The district is bounded on the north by and Khanewal and Sahiwal, on the east by Pakpattan, on the south by Bahawalpur and Bahawalnagar, on the west by Lodhran and Khanewal.

of

endmembers being derived, and the number of endmembers, estimated by an algorithm, with respect to the number of spectral bands, and the number of pixels being processed, also the required input data, and the kind of noise, if any, in the signal model surveying done. Results of the present study using the hyperspectral image analysis technique ascertain that Landsat ETM+ data can be used to generate valuable vegetative information for the District Vehari, Punjab Province, Pakistan.

*[Note: The effectiveness of the hyperspectral image analysis technique used in this study lies in their ability to compare a pixel spectrum with the spectra of known pure vegetation, extracted from the spectral endmember selection procedures, including the reflectance calibration of Landsat ETM+ image using ENVI software, minimum noise fraction (MNF), pixel purity index (PPI), and n-dimensional visualization. The Endmember extraction is one of the most fundamental and crucial tasks in hyperspectral data exploitation, an ultimate goal of an endmember extraction algorithm is to find the purest form of spectrally distinct resource information of a scene. The endmember extraction tendency to the type]*

Figure 13:

1

|   | Bands | nD Class 1-2 | nD Class 2-3 | nD Class 3-4 | nD Class 4-5 | nD Class 5-6 | nD Class 6-7 | nD Class 7-8 |
|---|-------|--------------|--------------|--------------|--------------|--------------|--------------|--------------|
| 1 |       | 81           | 74           | 75           | 84           | 74           | 76           | 76           |
| 2 |       | 68           | 62           | 62           | 84           | 61           | 64           | 66           |
| 3 |       | 78           | 66           | 67           | 99           | 69           | 74           | 75           |
| 4 |       | 70           | 57           | 68           | 77           | 71           | 86           | 64           |
| 5 |       | 255          | 103          | 255          | 48           | 255          | 255          | 109          |
| 8 |       | 1            | 255          | 255          | 38           | 1            | 1            | 255          |

Figure 14: Table 1 :

## 5 V. ACKNOWLEDGEMENTS

---

2

|   | Bands | nD         | Class 1-2 | nD | Class 2-3 | nD         | Class 3-4  | nD        | Class 4-5  | nD         | Class 5-6  | nD        | Class 6-7 | nD | Class 7-8  |            |
|---|-------|------------|-----------|----|-----------|------------|------------|-----------|------------|------------|------------|-----------|-----------|----|------------|------------|
| 1 | -     | -          | -         | -  | -         | -          | -          | -         | -          | -          | -          | -         | -         | -  | -          |            |
| 2 | -     | 45.668144  | 9.559686  | -  | 13.362324 | 42.251820  | 40.435787  | -         | 43.774044  | -          | 11.297052  | -         | -         | -  | -          |            |
| 3 | -     | 3.265855   | 0.914537  | -  | 18.957897 | -          | -          | 11.722809 | -          | 3.940382   | 14.638547  | 4.918655  | -         | -  | -          |            |
| 4 | -     | 15.752277  | -         | -  | -         | -          | -          | -         | -          | 20.311623  | 26.381514  | -         | -         | -  | -          |            |
| 5 | -     | 296.551239 | -         | -  | 29.919695 | 23.210220  | 2.429869   | -         | -          | 294.801758 | 282.927765 | -         | -         | -  | 31.349176  |            |
| 6 | -     | 139.244019 | -         | -  | 27.440727 | 146.126907 | 160.149399 | -         | 137.255051 | 48.182602  | 19.783876  | 24.758867 | -         | -  | -          | 135.733566 |
|   | -     | -          | -         | -  | -         | -          | -          | -         | 62.703640  | -          | -          | -         | -         | -  | 136.516922 |            |

Figure 15: Table 2 :

---

<sup>1</sup>© 2012 Global Journals Inc. (US) 20

<sup>2</sup>© 2012 Global Journals Inc. (US)

<sup>3</sup>© 2012 Global Journals Inc. (US) 20 2012

---

|              |  |
|--------------|--|
|              | purity index algorithm for remotely sensed hyperspectral image analysis, EURASIP Journal on Advances in Signal Processing, Vol. 2010, pp.1-13. doi: 10.1155/2010/969806.   |
| 19.          | GOP (2000). District census report of Vehari 1998, Population Census Organization, Statistics Division, Government of Pakistan, Islamabad, Pakistan, p.1.  |
| 20.          | Green AA, Berman M, Switzer P and Craig MD author wishes to thank his respected (1988). A transformation for ordering multispectral mentor Dr. Robert Bryant, Sheffield Centre for data in terms of image quality with implications for International Drylands Research, Department of noise removal, IEEE Transactions on Geoscience Geography, The University of Sheffield for review and and Remote Sensing, Vol. 26, pp.65-74. |
| Year         | providing valuable comments on draft-version of this paper.  |
| 2 30         | 21. Green RO, Eastwood ML and Sarture CM (1998). Imaging spectroscopy and the airborne References Références Referencias visible/infrared imaging spectrometer (AVIRIS), Volume 1. Aber JD and Martin ME (1995). High spectral resolution remote sensing of canopy chemistry, In: Summaries of the 5 th Annual JPL Airborne Issue  |
| W            |  |
| XV           |  |
| Ver-         |  |
| sion         |  |
| I            |  |
| D D          |  |
| D D          |  |
| ) A          |  |
| (            |  |
| Global Jour- | The spectral image processing system (SIPS) interactive visualization and analysis of imaging spectrometer data, Remote Sensing of Environment, nal of Human Social Science  |

Figure 16:



192 [Workshop ()] , Geoscience Workshop . <http://www.isprs.org/pdf> 2011. Oman. 10 p. . (Assessed on  
193 September)

194 [Boulder and Url (2011)] , C O Boulder , Url . <http://www.ittvis.com> November 28, 2011.

195 [Chang and Plaza ()] 'A fast iterative algorithm for implementation of pixel purity index'. C I Chang , A Plaza  
196 . 10.1109/LGRS.2005.856701. *IEEE Geoscience and Remote Sensing Letters* 2006. 3 (1) p. .

197 [Bateson and Curtiss ()] 'A method for manual endmember selection and spectral unmixing'. A Bateson , B  
198 Curtiss . *Remote Sensing of Environment* 1996. 55 p. .

199 [Chang et al. ()] 'A new growing method for simplex-based endmember extraction algorithm'. C I Chang , C C  
200 Wu , W W Liu , Y C Ouyang . *IEEE Transactions on Geoscience and Remote Sensing* 2006. 44 p. .

201 [Tu and Chang ()] 'A noise subspace projection approach to target signature detection and extraction in an  
202 unknown background for hyperspectral images'. T Tu , Chen C Chang , C . *IEEE Transactions on Geoscience  
203 and Remote Sensing* 1998. 36 (1) p. .

204 [Plaza et al. ()] 'A quantitative and comparative analysis of endmember extraction algorithms from hyperspectral  
205 data'. A Plaza , P Martinez , R Perez , J Plaza . *IEEE Transactions on Geoscience and Remote Sensing* 2004.  
206 42 (3) p. .

207 [Accessed on (2011)] [Acc essed on, acc.esa.gov/pub/docs/workshops/95\\_docs/1.PDF](http://acc.esa.gov/pub/docs/workshops/95_docs/1.PDF) . November 20, 2011.

208 [Welch et al. ()] 'ASTER as a source for topographic data in the late 1990's'. R Welch , T Jordan , Lang H  
209 Murakami , H . *IEEE Transactions on Geoscience and Remote Sensing* 1998. 36 p. .

210 [Boardman and Kruse ()] 'Automated spectral analysis: A geologic example using AVIRIS data, north Grapevine  
211 Mountains'. J W Boardman , F A Kruse . *Proceedings of 10th Thematic Conference on Geologic Remote  
212 Sensing*, (10th Thematic Conference on Geologic Remote SensingNevada; Ann Arbor, MI) 1994. I p. .  
213 Environmental Research Institute of Michigan

214 [Boardman (1993)] 'Automating spectral unmixing of AVIRIS data using convex geometry concepts'. J  
215 W Boardman . [ftp://popo.jpl.nasa.gov/pub/docs/workshops/93\\_docs/4.PDF](ftp://popo.jpl.nasa.gov/pub/docs/workshops/93_docs/4.PDF) . (Accessed on  
216 *Summaries of the 4 th Annual JPL Airborne Geoscience Workshop*, 1993. November 19. 2011. p. .

217 [Aspinall et al. ()] 'Considerations in collecting, processing, and analyzing high spatial resolution hyperspectral  
218 data for environmental investigations'. R J Aspinall , Marcus Wa , J W Boardman . *Journal of Geographical  
219 Systems* 2002. 4 p. .

220 [Tsai and Philpot ()] 'Derivative analysis of hyperspectral data'. F Tsai , W Philpot . *Remote Sensing of  
221 Environment* 1998. 66 p. .

222 [Earth Resources Observation and Science Center USGS (2008)] 'Earth Resources Observation and Science  
223 Center' . <http://glovis.usgs.gov/> USGS 2008. Accessed on December 04. 2008.

224 [Bateson et al. ()] 'Endmember bundles: A new approach to incorporating endmember variability into spectral  
225 mixture analysis'. A Bateson , G P Asner , C A Wessman . *IEEE Transactions on Geoscience and Remote  
226 Sensing* 2000. 38 (2) p. .

227 [Miao and Qi ()] 'Endmember extraction from highly mixed data using minimum volume constrained nonnegative  
228 matrix factorization'. L Miao , H Qi . *IEEE Transactions on Geoscience and Remote Sensing* 2007. 45  
229 p. .

230 [Exploring ENVI, Hyperion images ()] *Exploring ENVI, Hyperion images*, URL:[www.isprs.org/proceeding](http://www.isprs.org/proceeding)  
231 2004. Research System, Inc.

232 [González et al. ()] *FPGA implementation of the pixel p*, C González , J Resano , D Mozos , A Plaza , D Valencia  
233 . <ftp://popo.jpl.nasa.gov/pub/docs/workshop> 2010. p. 6.

234 [Sánchez and Plaza (2010)] *GPU implementation of the pixel purity index algorithm for hyperspectral people*  
235 *aplaza/Papers/Conferences/2010.Cluster.GP\_U.pdf*, S Sánchez , A Plaza . 2010. November 20, 2011.

236 [Roberts et al. ()] 'Green vegetation, non-photosynthetic vegetation, and soils in AVIRIS data'. D A Roberts ,  
237 Smith Mo , J B Adams . *Remote Sensing of Environment* 1993. 44 p. .

238 [Berman et al. ()] 'ICE: An automated statistical approach to identifying endmembers in hyperspectral images'.  
239 M Berman , H Kiiveri , R Lagerstrom , A Ernst , R Dunne , J Huntington . *IEEE Transactions on Geoscience  
240 and Remote Sensing* 2004. 42 p. .

241 [Goetz et al. ()] 'Imaging spectrometry for Earth remote sensing'. Afh Goetz , G Vane , J E Solomon , Rock Bn  
242 . 10.1126/science.228.4704.1147. *Science* 1985. 228 (4704) p. .

243 [Rogge et al. ()] 'Integration of spatial-spectral information for the improved extraction of endmembers'. D M  
244 Rogge , B Rivard , J Zhang , A Sanchez , Harris J Feng , J . *Remote Sensing of Environment* 2007. 110 p. .

245 [Shippert ()] *Introduction to hyperspectral* [al.ohio.edu/pdf/shippert.pdf](http://al.ohio.edu/pdf/shippert.pdf), P Shippert . 2003. 2011. 20.

246 [Rogge et al. ()] 'Iterative spectral unmixing for optimizing per-pixel endmember sets'. D M Rogge , B Rivard ,  
247 J Zhang , J Feng . *IEEE Transactions on Geoscience and Remote Sensing* 2006. 44 p. .

## 5 V. ACKNOWLEDGEMENTS

---

248 [Boardman (1998)] 'Leveraging the high dimensionality of AVIRIS data for improved sub-pixel target unmixing  
249 and rejection of false positives: Mixture Tuned Matched Filtering'. J W Boardman . *Summaries of the 7th*  
250 *Annual JPL Airborne Geoscience Workshop, ps/98\_docs/8.pdf*. (Accessed on, 1998. November 28, 201 1.

251 [Rn and Swayze ()] 'Mapping minerals, amorphous materials, environmental materials, vegetation, water, ice,  
252 and snow, and other materials: The USGS Tricorder Algorithm'. Clark Rn , G A Swayze . *Summaries of the*  
253 *5th Annual JPL Airborne Geoscience Workshop*, 1995. p. .

254 [Ben-Dor et al. ()] 'Mapping of several soil properties using DAIS-7915 hyperspectral scanner data: A case  
255 study over clayey soils in Israel'. E Ben-Dor , K Patkin , A Banin , A Karnieli . 10.1080/01431160010006962.  
256 *International Journal of Remote Sensing* 2002. 23 (6) p. .

257 [Boardman et al. (1995)] 'Mapping target signatures via partial unmixing of AVIRIS data'. J W Boardman  
258 , F A Kruse , R O Green . <http://trs-new.jpl.nasa.gov/dspace/bitstream/2014/33635/1/94-1613.pdf> *Summaries of the 5th Annual JPL Airborne Geoscience Workshop*, 1995. November 19. 201  
259 1. p. .

260 [Berk et al. ()] 'MODTRAN cloud and multiple scattering upgrades with application to AVIRIS'. A Berk , L S  
261 Bernstein , G P Anderson , P K Acharya , D C Robertson , J H Chetwynd , Adler-Golden Sm . *Remote*  
262 *Sensing of Environment* 1998. 65 p. .

263 [Tompkins et al. ()] 'Optimization of endmembers for spectral mixture analysis'. S Tompkins , J F Mustard , C  
264 M Pieters , D W Forsyth . *Remote Sensing of Environment* 1997. 59 p. .

265 [Mundt et al. (2007)] 'Partial unmixing of hyperspectral imagery: Theory and methods'. J T Mundt , D R  
266 Streutker , N F Glenn . <http://www.asprs.org/a/publications/proceedings/tampa2007/0046.pdf>. (Accessed on *Paper in ASPRS Annual Conference*, (Tampa, Florida) 2007. May 7-11, 2007. November  
267 28. 2011.

268 [Microimages (1999)] *Pixel purity index and masking aid endmember selection*, TNTmips, Inc Microimages  
269 . V6.10. <http://www.microimages.com/documentation/TechGuides/61Ppi.pdf>. (Accessed on  
270 1999. November 28, 2 011.

271 [Okin et al. ()] 'Practical limits on hyperspectral vegetation discrimination in arid and semiarid environments'.  
272 G S Okin , D A Roberts , B Burray , W J Okin . *Remote Sensing of Environment* 2001. 77 p. .

273 [Richards and Jia ()] *Remote sensing digital image analysis: An Introduction, Third Edition*, J A Richards , X  
274 Jia . 1999. Berlin: Springer-Verlag. p. .

275 [Plaza et al. ()] 'Spatial/spectral endmember extraction by multidimensional morphological operations'. A Plaza  
276 , P Martinez , R Perez , J Plaza . *IEEE Transactions on Geoscience and Remote Sensing* 2002. 40 p. .

277 [Qiu et al. ()] 'Spectral analysis of ASTER data covering part of the Neoproterozoic Allaqui-Heiani suture,  
278 Southern Egypt'. F Qiu , M Abdelsalam , P Thakkar . *Journal of African Earth Sciences* 2006. 44 p. .

279 [Song ()] 'Spectral mixture analysis for subpixel vegetation fractions in the urban environment: How to  
280 incorporate endmember variability'. C Song . *Remote Sensing of Environment* 2005. 95 p. .

281 [Zhang et al. ()] 'The successive projection algorithm (SPA), an algorithm with a spatial constraint for the  
282 automatic search of endmembers in hyperspectral data'. J Zhang , B Rivard , D M Rogge . *Sensors* 2008. 8  
283 p. .

284 [Al-Awadhi ()] *The use of remote sensing & geographical information systems to identify vegetation: The case of*, T Al-Awadhi , Al-Shukili A , Al-Amri Q . <http://dhofar/proceedings/2011/ISRSE34/211104015Final00239.p> 2011.

285 [Cochrane ()] 'Using vegetation reflectance variability for species level classification of hyperspectral data'. M A  
286 Cochrane . *International Journal of Remote Sensing* 2000. 21 (10) p. .

287 [Pal et al. ()] 'Utilization of Landsat ETM+ data for mineral-occurrences mapping over Dalma and Dhanjori'.  
288 S K Pal , T J Majumdar , A K Bhattacharya , R Bhattacharyya . *International Journal of Remote Sensing*  
289 2011. 32 (14) p. . (: An advanced spectral analysis approach)

290 [Mozaffar et al. (2008)] *Vegetation endmember extraction in s/XXXVII/congress/7\_pdf/3.../34.pdf*, M H Mozaf-  
291 far , Mjv Zoj , M R Sahebi , Y Rezaei . 2008. November 20, 2011.

292 [Nascimento and Dias ()] 'Vertex component analysis: A fast algorithm to unmix hyperspectral data'. Jmp  
293 Nascimento , Jmb Dias . 10.1109/TGRS.2005.844293. *IEEE Transactions on Geoscience and Remote Sensing*  
294 2005. 43 (4) p. .

295 [Shippert (2004)] *Why use hyperspectral imagery? Photogrammetric Engineering & Remote Sensing,*  
296 *~mignotte/IFT6150/ComplementCours/HyperspectralImagery.pdf*. (Accessed on, P Shippert . 2004. Novem-  
297 ber 20, 2011.

298 [Zhang et al. ()] B Zhang , X Wang , J Liu , L Zheng , Q Tong . *Hyperspectral image processing and analysis*  
299 *system (HIPAS) and its applications*, 2000. 66 p. .

300

301

302

303